Microwave spectroscopy of thermally excited quasiparticles in $YBa_2Cu_3O_{6.99}$

A. Hosseini, R. Harris, Saeid Kamal, P. Dosanjh, J. Preston,* Ruixing Liang, W. N. Hardy, and D. A. Bonn
Department of Physics and Astronomy, University of British Columbia, 6224 Agricultural Road, Vancouver, British Columbia, Canada V6T 1Z1

(Received 3 November 1998; revised manuscript received 29 January 1999)

We present here the microwave surface impedance of a high-purity crystal of $YBa_2Cu_3O_{6.99}$ measured at five frequencies between 1 and 75 GHz. This data set reveals the main features of the conductivity spectrum of the thermally excited quasiparticles in the superconducting state. Below 20 K there is a regime of extremely long quasiparticle scattering times, due to both the collapse of inelastic scattering below T_c and the very weak impurity scattering in the high-purity $BaZrO_3$-grown crystal used in this study. Above 20 K, the scattering increases dramatically, initially at least as fast as T^4. [S0163-1829(99)04425-2]

I. INTRODUCTION

Over the past few years measurements of electrodynamic properties at microwave frequencies have proven to be a fruitful technique for studying the superconducting state of the high-temperature superconductors. A key strength of the technique is that measurements of the real and imaginary part of the surface impedance $Z_s(\omega,T)$ provide complementary information on two aspects of the superconducting state; the superfluid density and the low-energy excitations out of the condensate.

Measurements of the imaginary part of the surface impedance $X_s(T)$ provide a direct measure of the penetration depth $\lambda(T)$, which is determined by the temperature dependence of the superfluid density. The widespread observation of a linear temperature dependence of $\lambda(T)$ at low T in many of the superconducting cuprates[1–5] has been a key piece of evidence suggesting nodes in the energy gap in these materials. Near T_c the temperature dependence of $\lambda(T)$ has provided evidence of $3DXY$ critical fluctuations over a wide temperature range in $YBa_2Cu_3O_{7-\delta}$.[6]

Measurements of the real part of the surface impedance $R_s(T)$, when combined with the measurements of $\lambda(T)$, can be used to determine the real part of the microwave conductivity $\sigma_1(T)$, which is essentially electromagnetic absorption by quasiparticles excited out of the condensate (either thermally excited quasiparticles or excitations created by the absorption of photons). Early measurements of $R_s(T)$ at a few GHz exhibited a broad peak below T_c, caused by a very large peak in $\sigma_1(T)$ (Ref. 7) at these low frequencies. This peak was also observed at THz frequencies by Nuss *et al.*,[8] and was attributed to a competition between two temperature dependences; the overall decrease with temperature of the number of thermally excited quasiparticles competing with a rapid increase below T_c of the transport scattering time of these quasiparticles. This rapid increase in scattering time has been interpreted as a collapse of the inelastic-scattering processes responsible for the large normal-state resistivity of the high-temperature superconductors and is an effect that is observed in thermal-conductivity measurements[9] as well as in other electromagnetic absorption measurements at microwave,[2,10–16] far infrared,[17] and THz frequencies.[8,18,19] The rapid increase in quasiparticle scattering time is well established by these measurements and the very long quasiparticle mean free paths resulting from this have been corroborated further by the thermal Hall-effect measurements of Krishana, Harris, and Ong.[20] However, obtaining a quantitative determination of the scattering time and the details of its temperature dependence has been hampered by the need to use models to interpret the existing microwave data. The problem has been that although the step from $R_s(T)$ and $\lambda(T)$ to the conductivity $\sigma_1(T)$ is a matter of straightforward superconductor electrodynamics when in the local limit, the extraction of a scattering time from $\sigma_1(T)$ suffered from a dependence on an assumed model for the shape of the quasiparticle conductivity spectrum $\sigma_1(\omega)$.

In this paper we present measurements at five microwave frequencies, giving enough spectroscopic detail over a wide enough frequency range to produce a rather complete picture of the evolution of $\sigma_1(\omega,T)$ in the superconducting state. These results support the early model based on an ansatz that the thermally excited quasiparticles have a Drude-shaped conductivity spectrum and now provide a much clearer measurement of the temperature dependence of the quasiparticle scattering rate below T_c. We find that this scattering rate becomes extremely small and appears to become essentially temperature independent below about 20 K. At higher temperatures the scattering rate increases rapidly, initially at least as fast as T^4. In the following section we will describe the techniques used to produce this information and in Sec. III we will present the results along with details of the extraction of the microwave conductivity from surface impedance measurements. In Sec. IV the microwave conductivity spectra will be presented along with the results of fits that generate the temperature dependence of the quasiparticle scattering rate. In Sec. V we will point out some of the implications of these results and in particular compare them to the present literature on conductivity in a *d*-wave superconductor.

II. EXPERIMENTAL TECHNIQUES

The property being directly probed in a microwave measurement on a superconductor is the complex surface impedance $Z_s(T)=R_s(T)+iX_s(T)$. One simplifying feature of the high-temperature superconductors is that the superfluid re-

sponse falls in the limit of local electrodynamics, so that $R_s(T)$ and $X_s(T)$ are related to the complex conductivity $\sigma(\omega,T)=\sigma_1(\omega,T)-i\sigma_2(\omega,T)$ in a straightforward way. This simple limit arises from the very small coherence length in these materials, which guarantees that $\xi \ll \lambda$. A particularly simple regime of the local limit occurs when $\sigma_2 \gg \sigma_1$ below T_c and at low frequency, in which case one obtains the relations

$$R_s(T)=\frac{\mu_0^2}{2}\omega^2\lambda^3(T)\sigma_1(\omega,T), \tag{2.1}$$

$$X_s(T)=\mu_0\omega\lambda(T).$$

A more detailed discussion of the electrodynamics and the extraction of $\sigma_1(\omega,T)$ from $Z_s(T)$ will be presented in Sec. III, but the equations above are useful for quick estimates and for understanding the main features of the microwave properties of these superconductors.

The expression for $R_s(T)$ in Eq. (2.1) embodies what is most difficult about the microwave measurements. It contains both σ_1 and a term of the form $\omega^2\lambda^3$, and physically can be interpreted as the microwave absorption processes (σ_1) occuring within the rather shallow depth into which the microwaves penetrate (hence the term $\omega^2\lambda^3$). This screening length set by the superfluid makes R_s extremely small below T_c, such that for small single crystals, one is forced to employ cavity perturbation in very high Q microwave resonators. This is most often achieved by the use of microwave cavities made from conventional superconductors cooled to low temperature. This fixed frequency type of measurement must be performed with several resonators if one is to build up a complete picture of the microwave conductivity spectrum $\sigma_1(\omega)$.

The data presented here involve measurements with five resonators spanning a 1–75 GHz range and utilizing a number of variations on the basic method of cavity perturbation. The common feature is that all of the measurements have been performed on the same sample, a thin plate of $YBa_2Cu_3O_{6.993}$ oriented such that the microwave magnetic field of each cavity lay in the plane of the plate ($\mathbf{H}_{rf}\|\hat{b}$). This geometry has the advantage that demagnetization factors are small, so the surface current distributions are fairly uniform and are similar in all of the measurements, making comparison from frequency to frequency quite reliable. The disadvantage is that although this geometry mainly measures the surface impedance for currents running across the crystal face in the $\hat{a}$ direction, there is some admixture of $\hat{c}$-axis surface impedance coming from currents running down the thin edge of the crystal. However, we have previously shown that these effects are small for a thin crystal, because the temperature dependences of $R_s(T)$ and $X_s(T)$ are quite weak in the $\hat{c}$ direction, except near T_c.[21,22] The absolute value of $R_s(T)$ for the $\hat{c}$ direction is also quite low.[22]

The measurements at 1 GHz were performed in a loop-gap resonator initially designed for measurement of $\lambda(T)$.[1] Like most of the resonators used in this study, the loop-gap is plated with a Pb:Sn alloy which is superconducting below 7 K and has very low microwave loss at 1.2 K. In the case of the 1-GHz loop-gap, the cavity Q can be as high as 4×10^6 at low temperature. Another feature common to all of the measurements is that the sample is mounted on a thin sapphire plate with a tiny amount of silicone grease, with the thermometry and sample heater located at the other end of the sapphire plate, outside of, and thermally isolated from the resonator. In this way the resonator can be held fixed at the regulated ^{4}He bath temperature while the sample temperature is varied. A unique feature of the 1-GHz loop-gap system is that the sample is held fixed in the resonator, with the sapphire plate and thermometry stage supported by a thin walled quartz tube which sustains the temperature gradient between the ^{4}He bath and the sample. This means that the sample cannot be removed from the resonator during the measurements, but we find this restriction is necessary for the high precision measurements of $\lambda(T)$ which rely on the sample being held rigidly in a position that does not vary when the temperature is changed. Without this type of construction, motion of the sample and sapphire plate in the fields of the resonator can give rise to experimental artifacts. This is because $\lambda(T)$ is determined from very small changes in the resonator frequency as the sample temperature is changed. This technique gives highly precise and reliable temperature dependences relative to the base temperature, but is limited to measuring differences; $\Delta\lambda(T)=\lambda(T)-\lambda(1.2\text{ K})$ and $\Delta R_s(T)=R_s(T)-R_s(1.2\text{ K})$. The value of $R_s(1.2\text{ K})$ at 1 GHz is estimated by comparing to separate experimental runs where the resonator is loaded with only the sapphire sample holder. The need to do this in two separate experimental runs gives the 1-GHz $R_s(T)$ measurements a relatively large uncertainty in the form of a temperature-independent background value ($\pm0.7\ \mu\Omega$), although the resolution of the temperature dependence is much better than this. We do not attempt to extract $\lambda(1.2\text{ K})$ from the microwave measurements, but instead use values inferred from muon spin rotation measurements.[23] None of the analysis discussed in this paper depends sensitively on this choice of $\lambda(1.2\text{ K})$.

The 2-GHz measurements have been performed in a Nb split-ring resonator that will be described in more detail elsewhere.[24] Measurements at 13.4, 22.7, and 75.3 GHz have been performed in the axial microwave magnetic fields of the TE_{011} modes of three right-circular cylindrical cavities. In all of the measurements other than those at 1 GHz, the sample can be easily moved in and out of the resonator. This freedom to move the sample makes it difficult to measure $\lambda(T)$ at the higher frequencies, due to problems of controlling motion of the sample as the temperature is changed. However, the sample motion is much too slight to have any influence on the measurements of $R_s(T)$. The ability to measure Q_0 by pulling the sample out rather than doing a separate experiment makes the background uncertainty in these measurements much less significant than it is in the 1-GHz data. The surface resistance is determined from $R_s(T)\propto 1/Q_s-1/Q_0$ where Q_0 is the Q of the empty cavity and Q_s is the Q with the sample inserted. A small correction for other sources of loss must be made by measuring the sapphire holder and grease without the sample. Then the only remaining uncertainty in the background is the influence of nonperturbative effects, which we check by measuring a superconducting Pb:Sn sample at 1.2 K. With these corrections, the estimated uncertainty in the background is 0.7, 0.2, 10, 20, and

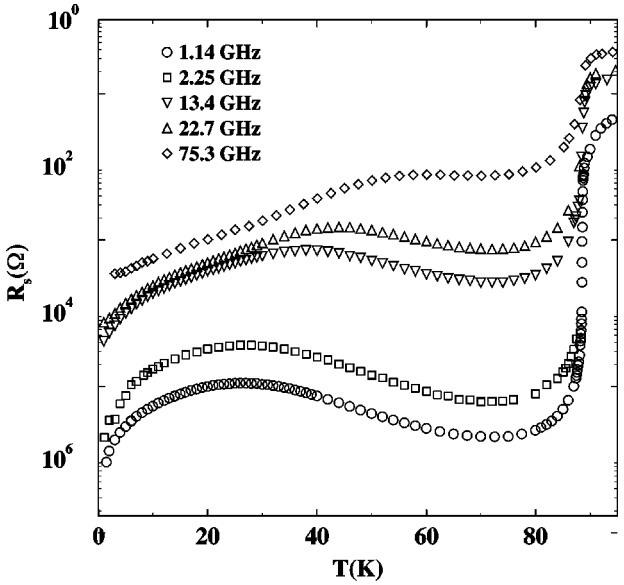

FIG. 1. The surface resistance $R_s(T)$ for currents running in the $\hat{a}$ direction of a high-purity crystal of $YBa_2Cu_3O_{6.993}$.

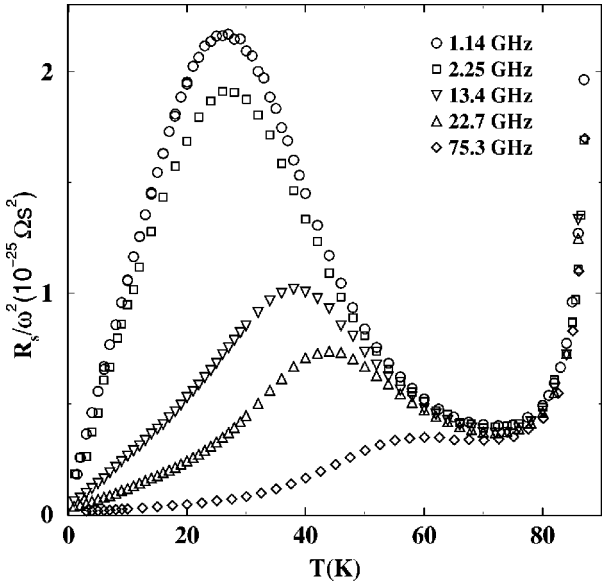

FIG. 2. The same measurements of surface resistance as shown in Fig. 1, but with the behavior below T_c emphasized by dividing out a frequency-squared dependence associated with superfluid screening.

360 $\mu\Omega$ for the 1.1, 2.2, 13.4, 22.7, and 75.3 GHz data, respectively. The calibration of the absolute value of the surface resistance is obtained by measuring a Pb:Sn reference sample whose normal-state surface resistance is governed by the classical skin effect. These calibrations, together with the statistical scatter in the data, amount to a total uncertainty of $\pm 10\%$ or less at each frequency.

The sample used for these measurements was a single crystal of $YBa_2Cu_3O_{6.993}$ grown by a flux growth technique using $BaZrO_3$ crucibles.[25] The $BaZrO_3$, which does not corrode during crystal growth, yields crystals of much higher purity[25,26] (better than 99.99%) than those grown in more commonly used crucibles such as yttria-stabilized zirconia and alumina. The sample was detwinned at 250 °C under uniaxial stress and then annealed at 350 °C for 50 days to produce a sample with nearly filled chain oxygen sites. This gives a slightly lower T_c (88.7 K) than the maximum obtained near an oxygen concentration of 6.91,[25] but provides particularly defect-free samples without the oxygen vacancy clustering discovered by Erb *et al.*[27] The dimensions of the sample were initially $2\times1\times0.02$ mm^3 for the 1-GHz measurements, which have been reported elsewhere.[28] Subsequent measurements in the other resonators were performed on smaller pieces cleaved from the original crystal, but measurements at 22.7 and 75.3 GHz were repeated on different pieces to ensure that the sample was uniform.

III. EXPERIMENTAL RESULTS AND ANALYSIS

Figure 1 shows the surface resistance of $YBa_2Cu_3O_{6.993}$ for currents running in the $\hat{a}$ direction. At all five of the frequencies shown in the figure, the rapid drop in $R_s(T)$ below T_c is due to the onset of screening by the superfluid, with the overall magnitude of the drop depending strongly on frequency as expected from the term in $R_s(T)$ that varies as $\omega^2\lambda^3(T)$. For easier comparison of the different frequencies, it is convenient to plot the low loss data in the superconducting state as R_s/ω^2 versus temperature, as shown in Fig. 2. One feature of these figures is that above 65 K the loss scales as ω^2 to within $\pm 8\%$, a scaling that is expected if the microwave $\sigma_1(\omega)$ is frequency independent above 65 K. This agreement lies within the estimated uncertainty in background and calibration constants, and provides a check of the degree to which one can compare the measurements at different frequencies.

The broad peak in $R_s(T)$ was originally attributed to a quasiparticle scattering time τ that increases rapidly with decreasing temperature below T_c and competes with a density of these thermally excited qusiparticles that decreases with temperature.[7] For the early measurements near 2 GHz it was suggested that the quasiparticle scattering time reaches a limiting value near 30 K, possibly due to impurity scattering, at which point the quasiparticle density takes over and causes $R_s(T)$ to fall again with further decreases in temperature.[29] The speculation that impurities are involved in the turnover at 30 K was partly checked by studying samples doped with Ni and Zn.[30] These doping studies showed either a smaller peak shifted to higher temperature or no peak at all, consistent with the quasiparticle scattering rate running into an impurity limit at higher temperature, even when only 0.15% Zn was added to the sample. This sensitivity to such low levels of impurities raises a serious concern over these earlier crystals grown in yttria-stabilized zirconia crucibles, because during crystal growth the residual impurity level due to uptake of material from the corroding crucible reaches the 0.1% level. The results shown here on a new higher purity sample confirm the original speculation that it is this residual impurity scattering that limits the increase in quasiparticle lifetime, even in quite pure crystals. The low-frequency surface resistance of the new crystal rises a factor of 4 above the minimum near 70 K, higher than the factor of 2 or less observed in earlier measurements of samples at 2 and 4 GHz.[29] The changes are consistent with the new samples having lower impurity scattering and so reaching a higher quasiparticle scattering time limit at a lower temperature than was

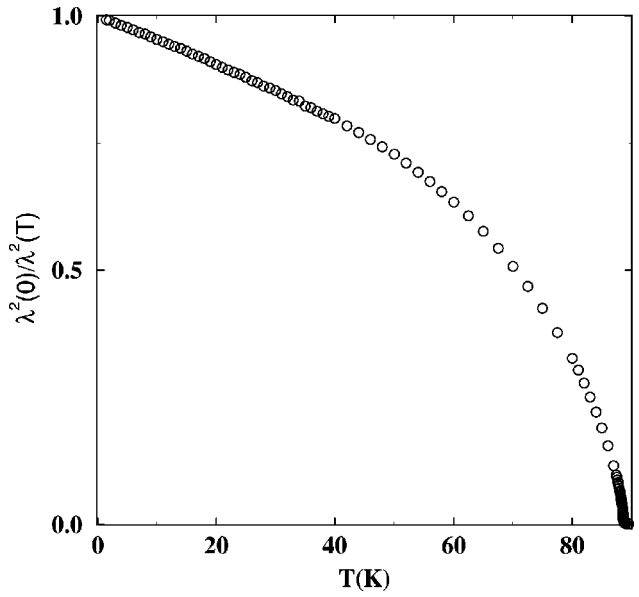

FIG. 3. The temperature dependence of the $\hat{a}$ axis penetration depth of $YBa_2Cu_3O_{6.95}$ plotted as $1/\lambda^2(T)$, which is a measure of the superfluid density via $n_s e^2/m^* = 1/(\mu_0 \lambda^2)$.

seen in the yttria-stabilized zirconia-grown crystals.

The frequency dependence of the peak in $R_s(T)$ provides further evidence of the rapid increase in the quasiparticle lifetime. In much higher frequency measurements on thin films, Nuss *et al.*[8] were the first to observe a similar broad peak in the THz range that shifted up in temperature and decreased in size at higher frequencies. They pointed out that this could be accounted for by relaxation effects. If the quasiparticle lifetime increases sufficiently that $\omega\tau \geqslant 1$, then the sample enters a regime where $\sigma_1(T)$ falls as τ continues to increase. So for high-frequency measurements the temperature at which $R_s(T)$ reaches its peak roughly indicates where $\omega\tau = 1$ at each measurement frequency. The fact that we observe these relaxation effects at 13 GHz indicates that the scattering time τ exceeds 10 ps in the new samples.

To better understand the data it is desirable to extract $\sigma_1(\omega, T)$ from these measurements of $R_s(\omega, T)$. At the lowest frequency of 1 GHz, where $\omega\tau \ll 1$ and we have simultaneous measurements of $R_s(T)$ and $\lambda(T)$, it is straightforward to extract $\sigma_1(T)$ with only an assumption that the electrodynamics are local. The 1-GHz measurements of $\lambda(T)$ used in this analysis are shown in Fig. 3, plotted as $1/\lambda^2(T)$. The screening by the superfluid follows the local London model if a superconductor is in the limit $\xi \ll \lambda$. Strictly speaking, this local limit is more complicated for the case of a superconductor with nodes in the energy gap because the coherence length is then k dependent and becomes large in the node directions. However, the consequences of this type of nonlocality for the electrodynamics would only be observable at low temperatures and the effect would be small in the measurement geometry used here.[31] A much more serious problem for the data analysis is that at the higher frequencies where $\omega\tau \geqslant 1$, the thermally excited quasiparticles also contribute to the screening of microwave fields and it is then incorrect to use the 1-GHz measurements of $\lambda(T)$ in order to extract $\sigma_1(T)$ from $R_s(T)$. Effectively, the penetration depth becomes frequency dependent, a phenomenon that has been observed directly in mm-wave measurements on particularly high quality thin films.[16] Ideally this problem can be solved by measuring both $R_s(T)$ and $X_s(T)$ at each measurement frequency, but we have done this only at 1 GHz, for reasons discussed in the previous section.

It is possible to work around the fact that we have measurements of both the real and imaginary part at only one frequency, as long as there is adequate information on the frequency dependence of the real part of the surface impedance. The problem is analogous to the one faced in far-infrared spectroscopy of opaque samples, where the reflectance, but not the phase of the reflected light, is measured over a wide frequency range. Kramers-Kronig relations are the usual solution if only one of the optical constants is known, but is known over a wide frequency range. In principle, data at the five microwave frequencies presented here could be connected to far-infrared measurements of reflectance in order to perform this analysis and extract $\sigma_1(\omega)$ and $\sigma_2(\omega)$. However, such an analysis is difficult because there still exists a substantial gap in the mm-wave frequency range between our highest frequency measurement and the lowest frequency far-infrared measurements on crystals. Some data have been obtained in the mm-wave region using techniques such as time domain THz measurements[8,18,19] and direct infrared absorption,[32] but these have all been performed on films rather than untwinned single crystals. The quasiparticle scattering rate is typically much higher in films than it is in single crystals, so data taken on such different samples cannot be analyzed together in this way. An alternative to a Kramers-Kronig analysis is to fit the frequency dependent surface resistance to a model, but this is not a very satisfactory procedure if one only has data at five microwave frequencies and one does not know the shape of the conductivity spectrum *a priori*. A further problem with both of these techniques is that the far-infrared data are only available at a couple of temperatures below T_c, so they cannot be used to do a complete analysis of the data presented here.

Our main approach to analyzing the surface resistance data is to use the $R_s(T)$ measurements at 1 GHz to arrive at an estimate of how much screening by the thermally excited quasiparticles must be included when extracting $\sigma_1(T)$ from $R_s(T)$ at higher frequencies. Although the procedure involves some assumptions about the model for the screening, we will show that the corrections are small enough that the effect of uncertainty in the choice of model does not significantly affect the conductivities that we extract in the analysis. We begin by writing down a general two-fluid expression for the microwave conductivity that includes contributions to the real and imaginary part from both the superfluid and normal fluid (the conductivity due mainly to thermally excited quasiparticles),

$$\sigma(\omega, T) = \sigma_{1S} - i\sigma_{2S} + \sigma_{1N} - i\sigma_{2N} = \pi \frac{n_s e^2}{m^*} \delta(\omega) - i \frac{n_s e^2}{m^* \omega} + \sigma_{1N} - i\sigma_{2N}, \quad (3.1)$$

where σ_{1S} and σ_{2S} are the real and imaginary parts of the superfluid conductivity and σ_{1N} and σ_{2N} are the real and imaginary parts of the normal-fluid conductivity. The superfluid contribution consists of a delta function at $\omega = 0$ with

an oscillator strength given by the superfluid density divided by the effective mass (n_s/m^*) and an imaginary part that is the inductive response of the superfluid at nonzero frequencies. This superfluid response can be expressed in terms of the penetration depth using $n_s e^2/m^* = [\mu_0 \lambda^2(T)]^{-1}$, and away from $\omega = 0$ the delta function can be neglected, leaving

$$\sigma(\omega,T) = \sigma_{1N}(\omega,T) - i\left[\sigma_{2N}(\omega,T) + \frac{1}{\mu_0 \omega \lambda^2(T)}\right]. \tag{3.2}$$

Thus, in general, the real part of the conductivity comes from the normal fluid. The imaginary part has contributions from both the normal and superfluid, although the superfluid dominates at low frequency.

In the local limit the connection between $\sigma_1(\omega,T)$ and the surface impedance is made via

$$Z_s = R_s + iX_s = \left(\frac{i\mu_0\omega}{\sigma_1 - i\sigma_2}\right)^{1/2}. \tag{3.3}$$

Thus at 1 GHz where we have measurements of both R_s and X_s, σ_1 and σ_2 can be extracted using

$$\sigma_1 = 2\mu_0\omega \frac{R_s X_s}{(R_s^2 + X_s^2)^2}, \tag{3.4}$$

$$\sigma_2 = \mu_0\omega \frac{X_s^2 - R_s^2}{(R_s^2 + X_s^2)^2}.$$

At higher frequencies, where we only have measurements of $R_s(T)$, it is useful to write σ_1 in terms of R_s and σ_2 in the following way:[29]

$$\sigma_1 = \left\{\left[\frac{\sigma_s}{2} \pm \left(\frac{\sigma_s^2}{4} - \sigma_2\sigma_s\right)^{1/2}\right]^2 - \sigma_2^2\right\}^{1/2} \tag{3.5}$$

with the sign choice $+(-)$ for $\sigma_1 > (<) \sqrt{3}\sigma_2$ and where $\sigma_s = \mu_0\omega/2R_s^2$. In the normal state, where $\sigma_1 \gg \sigma_2$ at low frequencies, this expression reduces to the classical skin effect result $\sigma_1 = \mu_0\omega/2R_s^2$. Equation (3.5) continues to be valid right through the superconducting transition and can be used to extract σ_1 from measurements of R_s provided that one also has some information on σ_2. The extent to which one can use this expression in the superconducting state depends upon the relative importance of the normal-fluid contribution to σ_2. In regimes where this contribution is small, σ_2 is simply given by $\sigma_{2S} = [\mu_0\omega\lambda^2(T)]^{-1}$ which can be calculated from the penetration depth measurements. To clearly illustrate the problem that occurs when the normal-fluid contribution to σ_2 is not small, we examine a particular version of the two-fluid model where the normal-fluid conductivity is assumed to have a Drude frequency dependence:

$$\sigma_{1N} - i\sigma_{2N} = \frac{n_n e^2}{m^*}\left[\frac{\tau}{1+(\omega\tau)^2} - i\frac{\omega\tau^2}{1+(\omega\tau)^2}\right], \tag{3.6}$$

where τ is the scattering time of the normal-fluid and n_n/m^* is the normal-fluid density over the effective mass. The ratio of the normal-fluid and superfluid contributions to the effective screening is then

$$\frac{\sigma_{2N}}{\sigma_{2S}} = \frac{n_n}{n_s}\frac{(\omega\tau)^2}{1+(\omega\tau)^2}. \tag{3.7}$$

The normal-fluid contribution to screening is thus unimportant at low frequency ($\omega\tau \ll 1$) or when the normal-fluid density is small ($n_n/n_s \ll 1$, which occurs at low temperatures). Conversely, difficulties arise when $\omega\tau > 1$ and n_n/n_s is not small, which is likely the case for our data at 13 and 22 GHz in the temperature range from 20–40 K, and for the 75-GHz data from 20–60 K.

For the conductivities that we will show below we take the following approach to estimating the normal-fluid contribution to σ_2. At 1 GHz σ_1 is calculated directly from the simultaneous measurements of $R_s(T)$ and $X_s(T)$. Then we extract an estimate of $\tau(T)$ using the Drude model above [Eq. (3.6)]. The normal-fluid density is calculated from the penetration depth measurements by assuming that

$$\frac{n_n e^2}{m^*}(T) + \frac{n_s e^2}{m^*}(T) = \frac{n_s e^2}{m^*}(T=0) \tag{3.8}$$

which amounts to assuming that all of the low-frequency oscillator strength is being shifted from the normal fluid to the superfluid as the temperature is decreased. The $\tau(T)$ and $n_n(T)$ derived from the 1-GHz data can then be used to make an estimate of the normal-fluid contribution to σ_2 needed to analyze the data at higher frequencies. When this analysis is performed, we find that the normal-fluid screening influences the extraction of σ_1 from $R_s(T)$ only at the level of 20% or less. This can be understood if one notices that $\omega\tau \sim 1$ at temperatures of 50 K or less at which point the normal-fluid density has already fallen below 20% of the total oscillator strength. There is some uncertainty associated with assuming a Drude form for $\sigma_1(\omega)$ [Eq. (3.6)] and assuming the redistribution of oscillator strength implied by the two-fluid model [Eq. (3.8)]. However, we will show that for temperatures up to 45 K, deviations from a Drude spectrum are barely discernible within our experimental uncertainties and the two-fluid model is obeyed at microwave frequencies to within 10%. Thus the maximum systematic error that might be introduced by this analysis amounts to 3% at worst at 75 GHz, only about 1% at 13 and 27 GHz, and is completely negligible at 1 and 2 GHz. Furthermore, the values of $\tau(T)$ that we use in the analysis above turn out to be consistent with the conductivity spectra $\sigma_1(\omega)$ that will be discussed below, so the correction for screening by the normal fluid is self-consistent.

Figure 4 shows the conductivities extracted from the $R_s(T)$ data of Fig. 1, using the methods described above. The sharp upturn at T_c marks the presence of superconducting fluctuations, which have been discussed in greater detail by Kamal *et al.*[6] and Pambianchi, Mao, and Anlage[33] and are not the main focus of the work presented here. A number of previous measurements on earlier generations of $YBa_2Cu_3O_{7-\delta}$ crystals have shown the presence of an extra sample-dependent peak in $\sigma_1(T)$ just below T_c, a feature that was discussed by Olson and Koch[34] and by Glass and Hall[35] who attributed it to having a sample with a broadened transition. A similar feature was also reported recently by Srikanth *et al.* for $BaZrO_3$-grown crystals,[36] but since we see no sign of this in our new high-purity samples, we conclude

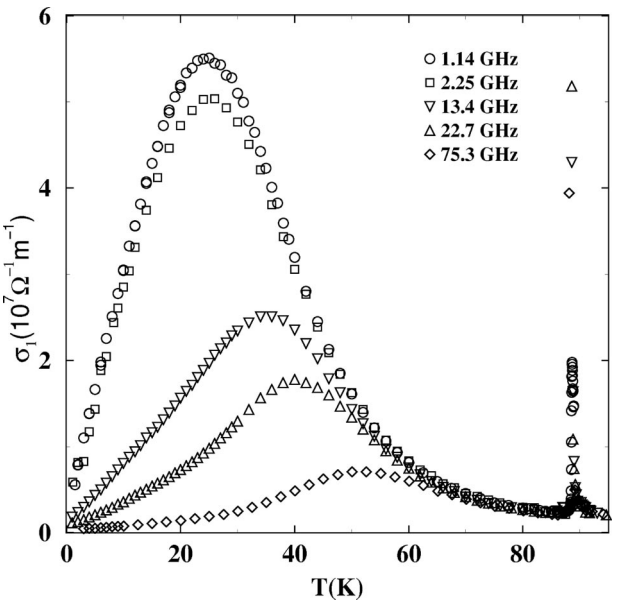

FIG. 4. The temperature dependence of the $\hat{a}$-axis microwave conductivity of $YBa_2Cu_3O_{6.993}$ extracted from the surface resistance measurements of Fig. 1. The sharp spike near T_c is a result of superconducting fluctuations and the broad peak at lower temperatures is caused by the increase in the scattering time of thermally excited quasiparticles.

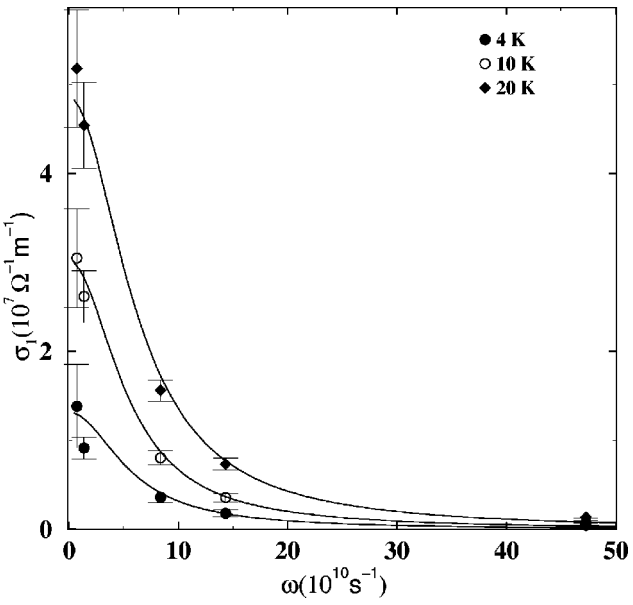

FIG. 5. The conductivity spectrum at three selected temperatures between 4 and 20 K, extracted from the $\sigma_1(T)$ curves of Fig. 4. In this temperature regime, the conductivity due to thermally excited quasiparticles has a nearly temperature-independent width of 9 ± 1 GHz and a nearly temperature-independent shape that is close to a Drude line shape (the lines are Drude fits).

that such features are associated with a spread in $T_c's$ in the surface of the sample. The main feature that we do observe in the conductivity is that $\sigma_1(T)$ has a large broad peak, rising to nearly 25 times the normal-state conductivity. The peak rises a factor of 2 higher than was seen in measurements at 2 and 4 GHz on an earlier generation of crystals grown in yttria-stabilized zirconia crucibles[30] and it crests at a lower temperature, 25 K instead of the 35 K turnover observed in the lower purity crystals. This effect of very low levels of impurities is not consistent with the suggestion of Klein[37] that this feature is the result of BCS-type coherence effects. A coherence peak, essentially a density-of-states effect, is observed near T_c in $\sigma_1(T)$ of *s*-wave superconductors such as Pb.[38] However, the peak observed here at 1 GHz is much too large and too low in temperature to be attributed to such an effect. Furthermore, a strong coherence peak has not been seen in NMR measurements of T_1 in this material[39] nor is it expected in a *d*-wave superconductor, the now widely accepted pairing state of $YBa_2Cu_3O_{7-\delta}$.[40,41]

Thus, in the absence of strong coherence effects, we have attributed the rise in $\sigma_1(T)$ below T_c to a rapid increase in the scattering time τ of thermally excited quasiparticles, as discussed in the Introduction. The fact that this peak rises higher and turns over at a lower temperature in the new, higher purity crystals is consistent with this interpretation. That is, in the higher purity sample, τ runs into its impurity limit at a somewhat lower temperature than it did in the earlier generations of crystals and this impurity-limited scattering time is very large in the new $BaZrO_3$-grown crystals. An estimate of the increase can be made as follows. The penetration depth measurements indicate that more than 90% of the normal-fluid density is gone at 25 K (see Fig. 3), so the 25-fold increase in σ_1 between T_c and 30 K implies an increase in τ by at least a factor of 250 over the scattering time just above T_c. This is actually an underestimate because not all of the far-infrared oscillator strength in the normal state ends up condensed into the superfluid at low temperatures. Such a huge increase in lifetime is consistent with the relaxation effects observed in the data at 13 GHz and higher. As a rough illustration of this agreement, far-infrared measurements indicate that $\omega\tau\sim1$ at about 3000 GHz just above T_c, so a 300-fold increase in τ below T_c would mean $\omega\tau\sim1$ at about 10 GHz, leading to the considerable frequency dependence in $\sigma_1(\omega)$ that we observe in the microwave range.

IV. CONDUCTIVITY SPECTRA AND QUASIPARTICLE LIFETIME

The evolution of the conductivity with temperature is better illustrated in Figs. 5 and 6 where we show the conductivity spectrum $\sigma_1(\omega)$ at several representative temperatures. In fact, the central technical achievement of this work is that we now have measurements at enough frequencies that both the shape of $\sigma_1(\omega)$ and its temperature dependence are quite clear. Figure 5 shows the conductivity spectrum at three temperatures below 25 K, the temperature range where we have argued above that the conductivity is dominated by thermally excited quasiparticles scattered by a low level of impurities. We will not concentrate here on the lowest temperature data, where the loss becomes very small and difficult to measure accurately by most cavity perturbation techniques. Figure 5 shows that from 4–20 K, the conductivity consists of a very narrow peak whose width is largely temperature independent. The lines in the figure are weighted, least-squares fits to a Lorentzian line shape [the real part of Eq. (3.6)], demonstrating that the conductivity spectrum of the thermally excited quasiparticles is Drude-like. The main contributions to

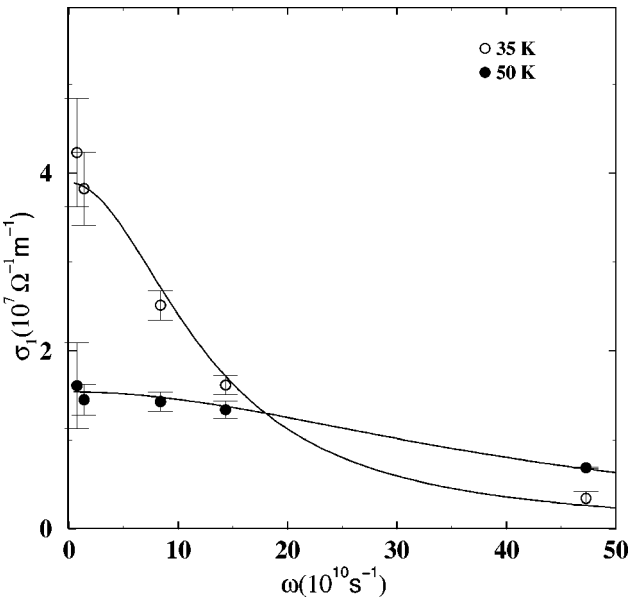

FIG. 6. The conductivity spectrum at two temperatures above 20 K, extracted from the $\sigma_1(T)$ curves of Fig. 4. Above 20 K, the width of the conductivity peak broadens rapidly, stretching out of the microwave frequency range above 55 K. These spectra continue to be reasonably well fit by Drude line shapes, as shown by the lines in the figure.

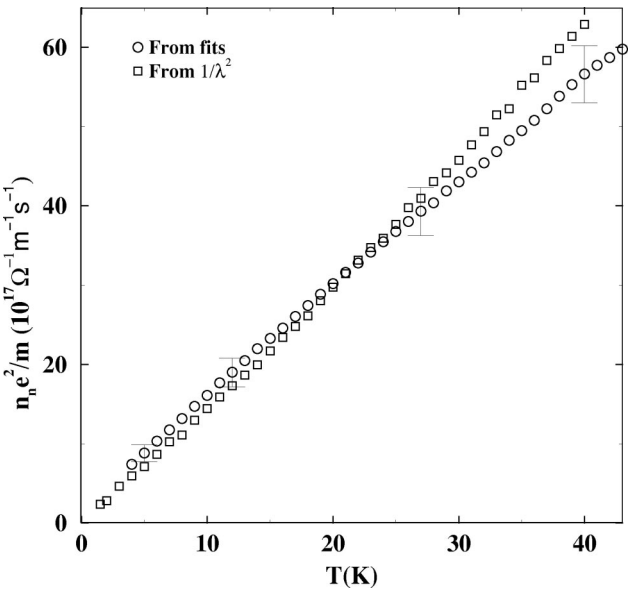

FIG. 7. A comparison of the normal-fluid oscillator strength determined in two ways: from Drude fits to spectra like those of Figs. 5 and 6 and from the disappearance of oscillator strength in the superfluid response, as measured by $1/\lambda^2$ (Fig. 3).

the error bars in these spectra are a combination of uncertainty in the individual measurements' calibration constants, plus a substantial uncertainty in the background loss in the 1.1-GHz measurements, and scatter in the 2.2-GHz measurements. Within these error estimates (mostly systematic error) there is very little clear deviation from a Drude line shape when examining an individual spectrum at a particular temperature. The most noticeable deviation is in the spectrum at 4 K, where the data may be taking on a slightly more cusp-like shape than the Drude curve. The nearly Lorentzian line shape largely confirms the ansatz originally used by Bonn *et al.*[29] to analyze the early $R_s(T)$ measurements.

An interesting crosscheck of these fits to $\sigma_1(\omega)$ is to compare the oscillator strength in the normal-fluid conductivity peak, which is given by the fit parameter $n_n e^2/m^*$, to the superfluid density $n_s e^2/m^* = (\mu_o \lambda^2)^{-1}$ extracted from the penetration depth measurements. If one assumes that all of the oscillator strength ends up in the superfluid δ function as $T \rightarrow 0$, then the superfluid density is related to the normal-fluid density via Eq. (3.8). Figure 7 shows a comparison between the normal-fluid density inferred from the fits to the $\sigma_1(\omega)$ peaks and the normal-fluid density inferred from the penetration depth via Eq. (3.8). This figure indicates that the normal-fluid density does nearly track the decline of the superfluid density with increasing temperature, which indicates that our use of a two-fluid model to describe the screening is a reasonable procedure. The increasingly serious deviation between the curves above 40 K is an indication that the Drude line shapes do not completely keep track of where all of the oscillator strength is going as temperature increases. There is also some deviation at low temperatures, taking the form of a normal-fluid oscillator strength that is extrapolating linearly towards a nonzero value as $T \rightarrow 0$. This is an indication of the presence of residual conductivity in the low-temperature, low-frequency limit, which is expected for a *d*-wave superconductor.[42]

The quality of the fits to $\sigma_1(\omega)$ and the agreement in the oscillator strengths shown in Fig. 7 indicate that the Drude fits do provide a reasonable measure of the width of the peaks from 4–45 K. The temperature dependent width coming from these fits, which we interpret as the scattering rate of the thermally excited quasiparticles, is shown in Fig. 8. One of the key results of these measurements is that the width of the normal-fluid peak is very small, 9 ± 1 GHz, and it is nearly temperature-independent up to 20 K. The main

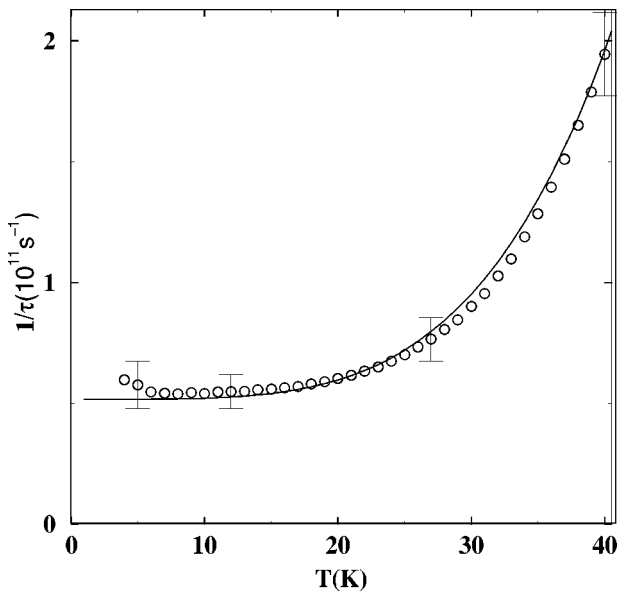

FIG. 8. The scattering rate of the thermally excited quasiparticles, as inferred from the width of Drude fits to the conductivity spectra of Figs. 5 and 6. The solid curve is a fit to a scattering rate that increases as $T^{4.2}$.

change in the spectra in this temperature range is an increase in oscillator strength, due to the shift of spectral weight from the superfluid response (a δ function at $\omega=0$) to the microwave conductivity. The narrow width suggests a very long quasiparticle scattering time of $1.8(\pm 0.2)\times 10^{-11}$ s.

One sees in Fig. 6 that above 25 K the conductivity peak broadens rapidly and by 60 K the width becomes much greater than the frequency range of the microwave measurements, so we have no direct measure of the width and shape of $\sigma_1(\omega)$ above 60 K. The exceptionally low level of defects in the new $BaZrO_3$-grown crystals, coupled with the measurements at five microwave frequencies, allows us to determine the temperature dependence of the inelastic scattering rate over a fairly wide temperature range from 20–40 K. Qualitatively similar results have been obtained in measurements on thin films by high-frequency microwave and THz techniques.[8,19] However, the much higher level of defects in such samples limits the temperature range over which the evolution of the inelastic-scattering rate can be observed. In the high-purity crystals, the temperature-dependent scattering can be tracked all the way down to 20 K. A fit to the form $1/\tau(T)=A+B(T/T_c)^y$ from 4–40 K yields an exponent $y=4.2\pm 0.1$, with coefficients $A=5.2(\pm 0.4)\times 10^{10}$ s^{-1} and $B=4.6(\pm 0.9)\times 10^{12}$ s^{-1}, and is shown as the solid curve in Fig. 8. The uncertainty in the exponent indicates the maximum range that is consistent with the data to within the estimated errors shown in Fig. 8.

V. DISCUSSION

For the purposes of discussing the data, we have divided the conductivity spectra up into the two regimes discussed in the previous section. In the range below about 20 K where the width of the peak in $\sigma_1(\omega)$ is narrow and nearly temperature independent, studies of samples over a wide range of purities indicate that this regime is governed by thermally excited quasiparticles being scattered by impurities or other defects.[30,50] Waldram *et al.* have pointed out the possibility that nonlocal effects might come into play in the conductivity in this regime, leading to an effective scattering rate that is not influenced by the density of residual impurities.[43] However, the considerable narrowing of $\sigma_1(\omega)$ that we have observed upon going from YSZ-grown crystals to the higher purity $BaZrO_3$-grown crystals indicates that the samples are still in a regime where impurities play a role in the low-frequency scattering. We have previously suggested an intuitively appealing way to interpret the spectra in this regime, based on a specific version of the two-fluid model.[29] In this phenomenological picture, the quasiparticles excited near the nodes in the energy gap have a temperature-independent scattering rate due to elastic scattering by impurities and a conductivity spectrum with a Drude line shape whose width is set by this scattering rate $1/\tau_i$ just like impurity scattering in a normal metal. In the high-purity samples this $1/\tau_i$ would correspond to a strikingly long mean free path of 4 μm if one takes the Fermi velocity to be $v_F=2\times 10^7$ cm/s. In this particular two-fluid model, the only source of temperature dependence in the low-temperature microwave conductivity is the density of the thermally excited quasiparticles, which increases linearly with temperature. This is a straightforward consequence of the linear dispersion of the gap function near the nodes and is also intimately connected to the linear temperature dependence of the penetration depth (they are Kramers-Kronig related).

Parameterizing the normal-fluid response in this way, with a temperature-dependent density and a scattering rate, has been partly justified by calculations of the microwave conductivity of a $d_{x^2-y^2}$ superconductor.[44] However, it is not so obvious that a temperature-independent scattering rate is expected for impurity scattering of these thermally excited quasiparticles near the nodes, since they differ greatly from free carriers at an ungapped Fermi surface. In particular, it has been pointed out by Hirschfeld and co-workers that elastic impurity scattering in this situation should lead to a frequency- and temperature-dependent scattering rate because of the restricted phase space into which the quasiparticles at the nodes can scatter.[44,46] So, with this possible conflict between theory and the phenomenological model in mind, we will make some more detailed comparison between the microwave conductivity data and the relevant theoretical calculations.

The transport properties (both microwave conductivity and thermal conductivity) of a $d_{x^2-y^2}$ superconductor have been the subject of considerable theoretical effort recently.[42,44–48] This work builds on earlier calculations of the transport properties of anisotropic superconductors, aimed primarily at explaining and predicting the properties of heavy fermion superconductors.[51,52] The high-temperature superconductors now offer an opportunity to test these calculations in a situation where we have a relatively simple anisotropic pairing state. Such comparisons are somewhat complex because the question of transport properties at low temperatures is inherently a question of understanding impurity effects. This is especially the case for anisotropic superconductors because the presence of impurities has a strong impact on the excitation spectrum near gap nodes, particularly in the limit of unitary scattering.

A key effect of impurities in an anisotropic superconductor is to produce a band of impurity states with a width γ, thus giving the superconductor a nonzero density of states at the Fermi level. One surprising consequence of these states is a universal conductivity limit at low frequency as $T\rightarrow 0$, first pointed out by P. A. Lee.[42] This residual conductivity is independent of impurity concentration, the result of a cancellation between the density of states induced by the presence of the impurities and the lifetime associated with those states. A version of this universal limit has been observed by Taillefer *et al.* in thermal-conductivity measurements of pure and Zn-doped $YBa_2Cu_3O_{6.9}$ below 1 K.[53] To the best of our knowledge, this limit has not yet been definitively observed in microwave conductivity measurements, in part due to sensitivity problems in the type of cavity perturbation measurement being discussed in this article. Instead, our main concern here will be the behavior of this conductivity as temperature and frequency are increased, which involves conductivities that are substantially larger than the $T\rightarrow 0$ limit and are thus easily measurable with the methods discussed above. This microwave conductivity has been the subject of considerable theoretical effort, including both numerical work and analytical results in certain limits.[44–48]

One well studied case involves the electrodynamic properties at temperatures and frequencies below the impurity

bandwidth γ, in the unitary scattering limit (scattering phase shift $\rightarrow \pi/2$). In this limit the impurity bandwidth is given roughly by $\gamma \sim (\Gamma\Delta)^{1/2}$ where Δ is the magnitude of the gap and Γ is the elastic-scattering rate that the impurities would contribute to the normal-state resistivity. For $\omega, T < \gamma$, where the transport properties are dominated by this impurity band, it has been shown that both σ_1 and λ vary as T^2.[44,45] This quadratic behavior has been seen in Zn-doped samples of $YBa_2Cu_3O_{6.95}$, where it was found that at a Zn impurity concentration as low as 0.15% the crossover energy scale is already $\gamma > 4$ K.[49,30] However, Zn substitution for planar Cu's is the only impurity that we have found that clearly gives this unitary scattering behavior. Ni substitution for Cu, Ca substitution for Y, and the chain oxygen vacancies all have much weaker effects, even at defect levels of 1% or more.[21] The previous generation of YSZ-grown crystals showed only slight curvature in $\lambda(T)$ and $\sigma_1(T)$ below 4 K and the new $BaZrO_3$-grown crystals show no hint of T^2 temperature dependence down to 1.2 K. The relative rarity of T^2 behavior (though it is common in films for reasons that remain unclear[54]) leads us to consider the opposite limit for the strength of the scattering, the Born limit.

For impurity scattering in the Born limit, the crossover energy scale is exponentially small, so one does not expect to see the universal conductivity limit until measurements are performed well below 1 K. In fact, in the microwave measurements presented here we are also not necessarily at low enough *frequency* to observe any simple limiting behavior. So, we compare our results qualitatively to numerical calculations performed in the Born limit by Hirschfeld, Putikka, and Scalapino.[46] They found that at very low frequency $\sigma_1(T)$ rises rapidly from the universal zero-temperature limit to a much larger conductivity that depends upon the impurity scattering rate. It remains fairly temperature independent until inelastic-scattering processes become important. At higher frequencies $\sigma_1(T)$ becomes smaller and moves through a whole range of behaviors, varying from mostly sublinear in T at low frequency, through a quasilinear temperature dependence at intermediate frequencies, to a faster than linear temperature dependence at high frequencies. Figure 9 shows behavior in the measured microwave conductivity that is similar to this Born limit result in some of its qualitative features. The overall conductivity has a magnitude that varies with purity, from the quite high values seen here, through to very low, flat conductivities observed in Ni-doped samples.[30] More importantly, here we do clearly see that the linear behavior of $\sigma_1(T)$ is an intermediate behavior, albeit one that survives over a substantial range of frequency and temperature. The evolution in the shape of $\sigma_1(T)$ at low T clearly falls outside of our phenomenological model, which would have predicted a linear temperature dependence at all of the frequencies shown in Fig. 9. That is, if $\sigma_1(\omega)$ were really Drude shaped with a temperature-independent width, then $\sigma_1(T)$ would exhibit the same temperature dependence at all frequencies; namely, the linear temperature dependence of the normal-fluid density.

At our lowest frequencies the data does move towards sublinear as expected in the Born limit. However, one perhaps important difference from the theoretical calculations is that the trend does not to continue below 2 GHz. The data stops evolving towards the expected low-frequency behavior,

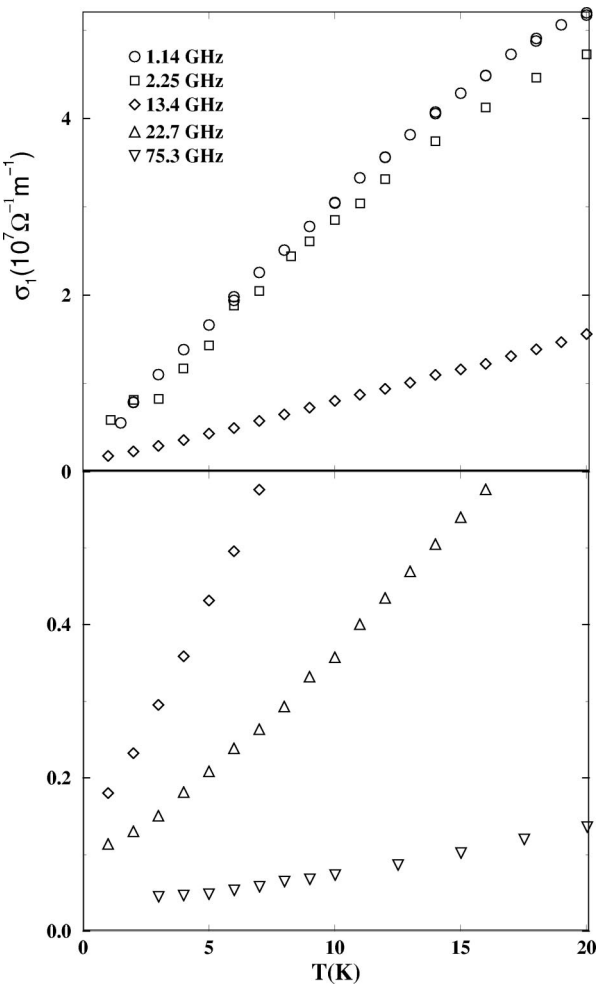

FIG. 9. This detailed view of the temperature dependence of the microwave conductivity below 20 K shows a gradual evolution of the shape of of $\sigma_1(T)$, from concave up at high frequencies to concave down at the lowest frequencies. The quite linear temperature dependence seen here at 13 GHz seems to be an intermediate behavior.

which is a rapid leap upwards to a constant value. The reason for this is not yet clear, so we are left for the moment with qualitative features that seem only weakly in accord with Born limit scattering. Other features of the data echo the expectations of a conductivity spectrum with a Drude-like line shape that has a temperature-independent width; namely, the similarity in the 1 and 2 GHz curves and the relatively large frequency and temperature range over which $\sigma_1(T)$ is nearly linear in T. It is the latter aspects of the data that lead to the Drude model being a fairly good description of the conductivity spectra.

Although the foregoing discussion indicates that the $\sigma_1(\omega)$ spectra cannot be perfectly Drude shaped, there is still a characteristic width to the peaks that is well parameterized by the Drude fits. Thus the plot of scattering rates shown in Fig. 8 provides a reasonable measure of the narrowness of the peak at low temperature and its rapid broadening above 20 K. Just above 20 K, the initial onset of this increase in scattering appears to be at least as rapid as T^4 and must rise even more quickly at higher temperatures in order to meet the width observed in the normal-state far-infrared measurements. A rapid temperature dependence of the qua-

siparticle scattering time would be expected in any situation where the inelastic scattering comes from interactions that become gapped below T_c. A number of early calculations tackled the problem of the collapse of the scattering rate below T_c in this way. Early on, Nuss *et al.* explained the peak in their THz conductivity measurements in this manner.[8] Littlewood and Varma studied this type of effect in a marginal Fermi liquid,[55] the idea being that below T_c a gap opens up in the scattering spectrum. Statt and Griffin similarly studied the effect of the opening of a gap in the spectrum of spin fluctuations.[56] All of this work predated the solid identification of the $d_{x^2-y^2}$ pairing state, so isotropic *s*-wave gaps were assumed in the calculations. Quinlan, Scalapino, and Bulut studied a model in which quasiparticle lifetimes were associated with spin-fluctuation scattering. They studied the effects of both *s*-wave and *d*-wave gaps opening up in the spin-fluctuation spectrum.[57] Since we now know that the gap in this material has $d_{x^2-y^2}$ symmetry, this latter calculation is most directly relevant to our measurements here. In particular they found that at temperatures well below T_c, the quasiparticle lifetime increases as T^3 and even faster than this as T_c is approached. In a comparable temperature range, the transport scattering rate that we extract from the width of $\sigma_1(\omega)$ is closer to T^4. Thus the temperature dependence of the inelastic-scattering rate seems to be about one power of T faster than the lifetime calculations based on a gapping of the spin-fluctuation spectrum. One must note, however, that the quasiparticle lifetime can in principle differ from the electronic transport scattering time, since charge transport is most strongly affected by backscattering.

VI. CONCLUSIONS

We have presented here complete microwave measurements on a crystal of a high-temperature superconductor. These spectra reveal a wealth of detail regarding the conductivity spectrum $\sigma_1(\omega)$ of the thermally excited quasiparticles in the superconducting state. We find that $\sigma_1(\omega)$ has a Drude-like shape. Although in detail there may be deviations from this shape, there is nevertheless a well defined characteristic width which can be associated with the transport scattering time of the quasiparticles. Below T_c the width collapses rapidly and it becomes easily discernible in the microwave spectral range at temperatures below 55 K. In the range between 45 and 20 K we find that the collapse of the scattering rate varies at least as fast as T^4. By 20 K the width becomes extremely narrow and nearly temperature independent. This narrow width of only 9 GHz corresponds to a mean free path as high as 4 μm if we interpret the width as being a direct measure of the elastic-scattering rate due to impurities. We find that some features of $\sigma_1(\omega,T)$ below 20 K are in accord with quasiparticle scattering in the Born limit for a $d_{x^2-y^2}$ superconductor, in particular, a gradual evolution of the shape of $\sigma_1(T)$ from sublinear T dependence at low ω, to quasilinear and then faster at higher ω. However, there remain discrepancies that might best be settled by a detailed numerical calculation aimed at fitting the observations presented here. Such fits must come to grips with the observation that the behavior of $\sigma_1(\omega,T)$ below 20 K is reasonably well described by a model involving quasiparticle scattering with a temperature-independent scattering rate.

ACKNOWLEDGMENTS

We are greatly indebted to A. J. Berlinsky and C. Kallin for many helpful discussions regarding transport properties in *d*-wave superconductors. We wish also to acknowledge helpful conversations with D. J. Scalapino, P. J. Hirschfeld, P. A. Lee, and G. Sawatsky, and are grateful for the opportunity to carry out some of this work at the Aspen Center for Physics. We also thank J. Trodahl for his contribution to the design of the 75-GHz-cavity setup. This research was supported by the Natural Science and Engineering Research Council of Canada and the Canadian Institute for Advanced Research. D.A.B. acknowledges support from the Sloan Foundation.

*Permanent address: Dept. of Physics and Astronomy, McMaster University, 1080 Main St. W, Hamilton, ON, Canada, L8S 4M1.

[1] W. N. Hardy, D. A. Bonn, D. C. Morgan, Ruixing Liang, and Kuan Zhang, Phys. Rev. Lett. **70**, 3999 (1993).

[2] D. M. Broun, D. C. Morgan, R. J. Ormeno, S. F. Lee, A. W. Tyler, A. P. MacKenzie, and J. R. Waldram, Phys. Rev. B **56**, 11 443 (1997).

[3] L. A. de Vaulchier, J. P. Vieren, Y. Guldner, N. Bontemps, R. Combescot, Y. Lemaitre, and J. C. Mage, Europhys. Lett. **33**, 153 (1996).

[4] Shih-Fu Lee *et al.*, Phys. Rev. Lett. **77**, 735 (1996).

[5] T. Jacobs, S. Sridhar, Qiang Li, G. D. Gu, and N. Koshizuka, Phys. Rev. Lett. **75**, 4516 (1995).

[6] S. Kamal, D. A. Bonn, Nigel Goldenfeld, P. J. Hirschfeld, R. Liang, and W. N. Hardy, Phys. Rev. Lett. **73**, 1845 (1994).

[7] D. A. Bonn, P. Dosanjh, R. Liang, and W. N. Hardy, Phys. Rev. Lett. **68**, 2390 (1992).

[8] Martin C. Nuss, P. M. Mankiewich, M. L. O'Malley, E. H. Westerwick, and Peter B. Littlewood, Phys. Rev. Lett. **66**, 3305 (1991).

[9] R. C. Yu, M. B. Salamon, J. P. Lu, and W. C. Lee, Phys. Rev. Lett. **69**, 1431 (1992).

[10] T. Shibauchi, A. Maeda, H. Kitano, T. Honda, and K. Uchimokura, Physica C **203**, 315 (1992).

[11] Jian Mao, D. H. Wu, J. L. Peng, R. L. Greene, and Steven M. Anlage, Phys. Rev. B **51**, 3316 (1995).

[12] Kuan Zhang, D. A. Bonn, S. Kamal, Ruixing Liang, D. J. Baar, W. N. Hardy, D. Basov, and T. Timusk, Phys. Rev. Lett. **73**, 2484 (1994).

[13] Steven M. Anlage, Dong-Ho Wu, J. Mao, S. N. Mao, X. X. Xi, T. Venkatesan, J. L. Peng, and R. L. Greene, Phys. Rev. B **50**, 523 (1994).

[14] T. Shibauchi, H. Kitano, K. Uchinokura, A. Maeda, T. Kimura, and K. Kishio, Phys. Rev. Lett. **72**, 2263 (1994).

[15] H. Kitano, T. Shibauchi, K. Uchinokura, A. Maeda, H. Asaoka, and H. Takei, Phys. Rev. B **51**, 1401 (1995).

[16] U. Dahne, Y. Goncharov, N. Klein, N. Tellmann, G. Kozlov, and K. Urban, J. Supercond. **8**, 129 (1995).

[17] D. B. Romero, C. D. Porter, D. B. Tanner, L. Forro, D. Mandrus, L. Mihaly, G. L. Carr, and G. P. Williams, Phys. Rev. Lett. **68**, 1590 (1992).

[18] S. Spielman, Beth Parks, J. Orenstein, D. T. Nemeth, John Clarke, Paul Merchant, and D. J. Lew, Phys. Rev. Lett. **73**, 1537 (1994).
[19] A. Pimenov, A. Loidl, G. Jakob, and H. Adrian (unpublished).
[20] K. Krishana, J. M. Harris, and N. P. Ong, Phys. Rev. Lett. **75**, 3529 (1995).
[21] W. N. Hardy *et al.*, *Proceedings of the 10th Anniversary HTS Workshop* (World Scientific, Singapore, 1996); D. A. Bonn *et al.*, *Proceedings of the 21st Low Temperature Physics Conference* [Czech. J. Phys. **46**, 3195 (1996)].
[22] A. Hosseini, Saeid Kamal, D. A. Bonn, Ruixing Liang, and W. N. Hardy, Phys. Rev. Lett. **81**, 1298 (1998).
[23] J. L. Tallon, C. Bernhard, U. Binninger, A. Hofer, G. V. M. Williams, E. J. Ansaldo, J. I. Budnick, and Ch. Niedermayer, Phys. Rev. Lett. **74**, 1008 (1995).
[24] B. Gowe, P. Dosanjh, and D.A. Bonn (unpublished).
[25] Ruixing Liang, D. A. Bonn, and W. N. Hardy, Physica C **304**, 105 (1998).
[26] A. Erb, E. Walker, and R. Flukiger, Physica C **245**, 9 (1996).
[27] A. Erb, J. Y. Genoud, F. Marti, M. Daumling, E. Walker, and R. Flukiger, J. Low Temp. Phys. **105**, 1023 (1996).
[28] S. Kamal, Ruixing Liang, A. Hosseini, D. A. Bonn, and W. N. Hardy, Phys. Rev. B **58**, 8933 (1998).
[29] D. A. Bonn, Ruixing Liang, T. M. Riseman, D. J. Baar, D. C. Morgan, K. Zhang, P. Dosanjh, T. L. Duty, A. MacFarlane, G. D. Morris, J. H. Brewer, W. N. Hardy, C. Kallin, and A. J. Berlinsky, Phys. Rev. B **47**, 11 314 (1993).
[30] D. A. Bonn, S. Kamal, Kuan Zhang, Ruixing Liang, D. J. Baar, E. Klein, and W. N. Hardy, Phys. Rev. B **50**, 4051 (1994).
[31] Ioan Kosztin and Anthony J. Leggett, Phys. Rev. Lett. **79**, 135 (1997).
[32] D. Miller, P. L. Richards, S. Etemad, A. Inam, T. Venkatesan, B. Dutta, X. D. Wu, C. D. Eom, T. H. Gebake, N. Newman, and B. F. Cole, Phys. Rev. B **47**, 8076 (1993).
[33] M. S. Pambianchi, S. N. Mao, and S. M. Anlage, Phys. Rev. B **52**, 4477 (1995).
[34] H. K. Olson and R. H. Koch, Phys. Rev. Lett. **68**, 2406 (1992).
[35] N. E. Glass and W. F. Hall, Phys. Rev. B **44**, 4495 (1991).
[36] H. Srikanth, B. A. Willemsen, T. Jacobs, S. Sridhar, A. Erb, E. Walker, and R. Flukiger, Phys. Rev. B **55**, 14 733 (1997).
[37] O. Klein, Phys. Rev. Lett. **72**, 1390 (1994).
[38] K. Holczer, O. Klein, and G. Gruner, Solid State Commun. **78**, 875 (1991).
[39] P. C. Hammel, M. Takigawa, R. H. Heffner, Z. Fisk, and K. C. Ott, Phys. Rev. Lett. **63**, 1992 (1989).
[40] D. J. Scalapino, in *High Temperature Superconductivity*, edited by K. S. Bedell, D. Coffey, D. Meltzer, D. Pines, and J. R. Schrieffer (Addison-Wesley, Reading, MA, 1990).
[41] N. Bulut and D. J. Scalapino, Phys. Rev. Lett. **68**, 706 (1992).
[42] P. A. Lee, Phys. Rev. Lett. **71**, 1887 (1993).
[43] J. R. Waldram, P. Theopistou, A. Porch, and H.-M. Cheah, Phys. Rev. B **55**, 3222 (1997).
[44] P. J. Hirschfeld, W. O. Putikka, and D. J. Scalapino, Phys. Rev. Lett. **71**, 3705 (1993).
[45] Peter J. Hirschfeld and Nigel Goldenfeld, Phys. Rev. B **48**, 4219 (1993).
[46] P. J. Hirschfeld, W. O. Putikka, and D. J. Scalapino, Phys. Rev. B **50**, 10 250 (1994).
[47] D. Xu, S. K. Yip, and J. A. Sauls, Phys. Rev. B **51**, 16 233 (1995).
[48] S. Hensen, G. Muller, C. T. Rieck, and K. Scharnberg, Phys. Rev. B **56**, 6237 (1997).
[49] D. Achkir, M. Poirier, D. A. Bonn, Ruixing Liang, and W. N. Hardy, Phys. Rev. B **48**, 13 184 (1993).
[50] Kuan Zhang, D. A. Bonn, Ruixing Liang, D. J. Baar, and W. N. Hardy, Appl. Phys. Lett. **62**, 3019 (1993).
[51] P. J. Hirschfeld, P. Wolfle, J. A. Sauls, D. Einzel, and W. O. Putikka, Phys. Rev. B **40**, 6695 (1989).
[52] R. A. Klemm, K. Scharnberg, D. Walker, and C. T. Rieck, Z. Phys. B **72**, 139 (1988).
[53] Louis Taillefer *et al.*, Phys. Rev. Lett. **79**, 483 (1997).
[54] D. A. Bonn and W. N. Hardy, in *Physical Properties of High Temperature Superconductors*, edited by D. M. Ginsberg (World Scientific, Singapore, 1996), Vol. V.
[55] P. B. Littlewood and C. M. Varma, Phys. Rev. B **46**, 405 (1992).
[56] B. W. Statt and A. Griffin, Phys. Rev. B **46**, 3199 (1992).
[57] S. M. Quinlan, D. J. Scalapino, and N. Bulut, Phys. Rev. B **49**, 1470 (1994).